Journal of Molecular Structure 1252 (2022) 132101

Contents lists available at ScienceDirect

Journal of Molecular Structure

journal homepage: www.elsevier.com/locate/molstr

Study of new Zn(II)Prolinedithiocarbamate as a potential agent for breast cancer: Characterization and molecular docking

Rizal Irfandi[a,b], Santi Santi[c], Indah Raya[d,*], Ahyar Ahmad[d], Ahmad Fudholi[e,f], Dewi Ratih Tirto Sari[g], Prihantono[h]

[a] Doctoral Program, Department of Chemistry, Faculty of Mathematics, and Natural Science, Hasanuddin University, Makassar 90245, Indonesia
[b] Department of Biology Education, Faculty of Teacher Training and Education, Universitas Puangrimaggalatung, Sengkang 90915, Indonesia
[c] Medical Laboratory Technology, Faculty of Health Technology, Megarezky University, Makassar 90234, Indonesia
[d] Department of Chemistry, Faculty of Mathematics, and Natural Science, Hasanuddin University Makassar 90245, Indonesia
[e] Solar Energy Research Institute, Universiti Kebangsaan Malaysia, UKM Bangi, Selangor 43600, Malaysia
[f] Research Centre for Electrical Power and Mechatronics, Institute of Science (LIPI), Bandung, Indonesia
[g] Research Center of Smart Molecules and Natural Genetic Resources, Brawijaya University, Malang, Indonesia
[h] Department of Surgery, Faculty of Medical, Hasanuddin University, Makassar 90245, Indonesia

ARTICLE INFO

Article history:
Received 17 October 2021
Revised 26 November 2021
Accepted 5 December 2021
Available online 7 December 2021

Keywords:
Dithiocarbamate
DNA
MCF-7
Molecular docking
In vitro

ABSTRACT

This study characterized the synthetic Zn(II)Prolinedithiocarbamate and determined its anti-cancer activity in vitro and in silico. Zn(II)Prolineditiocarbamate complex was synthesized, characterized, and determined by melting point, conductivity value, UV–Vis spectroscopy, FT-IR and XRD. Computational NMR spectrum analysis has been carried out. Zn(II)Prolinedithiocarbamate complex's binding to DNA was studied using an in vitro molecular docking anti-cancer activity assay. Molecular docking results showed the interaction of Zn(II)Prolinedithiocarbamate complex with DNA from MCF-7 strain cells. Cytotoxicity of Zn(II)Prolinethiocarbamate against the MCF-7 cell line showed changes in cancer cell morphology at an IC50 value of 360.10 g/mL. Zn(II)Prolinedithiocarbamate complex compounds can be a breakthrough in developing chemotherapy drugs that are potential and effective against the MCF-7 cell line.

1. Introduction

Cancer arises due to genetic changes that occur in the DNA structure of cancer cells so that the growth of abnormal cells impacts the function of tissues and organs of the body [1–3]. Until recently, cancer was one of the top causes of mortality around the globe. Based on data from the Global Burden of Cancer (GLOBOCAN) in 2018, breast cancer has the highest mortality rate and prevalence in Indonesia. New cases of breast cancer 58,256 people (16.7%) with the number of deaths 22,692 people (11%), it is estimated that the number of new cases and deaths will continue to increase in the next two decades [4]. Chemotherapy becomes an essential treatment for breast cancer. FDA approved breast cancer treatment in the form of Fulvestrant agent functioning as a down-regulating agent of selective estrogen receptors encapsulated in silica nanocapsules (SNC) biopolymers [5] and Using layer-by-layer (LBL) self-assembly technology, hyaluronic acid biopolymers were used to produce a sandwich-like membrane based on hydrogen bonding. The multilayer films absorbed osimertinib, a third-generation inhibitor for the treatment of nonsmall cell lung cancer (NSCLC), effectively [6].

Chemotherapy and metal-based drugs have become viable research areas in medicinal chemistry after the unexpected discovery of the coordination compound cisplatin [7,8]. Cisplatin is a platinum-based drug for cancer therapy. However, cisplatin drugs still have some drawbacks such as lack of selectivity, unfavorable side effects, resistance, and toxicity in the body, which encourage the search for efficient and selective non-platinum drugs [9,10]. The design of new therapeutic agents is of great importance for chemical medicine Metal complexes have become one of the latest cancer chemotherapeutic medication finding methodologies. Metal complexes are reported to have biological activities such as antioxidant, antimicrobial, antimalarial, and anti-cancer. This is related to the synergistic relationship between the ligand and the central metal [11]. The transition metal complexes Ni, Cu, and Zn, showed

* Corresponding author.
E-mail address: indahuh17@gmail.com (I. Raya).

https://doi.org/10.1016/j.molstruc.2021.132101
0022-2860/

significantly better cytotoxicity than cis-platin-based drugs. Zinc (Zn) actively participates in more than 200 enzymatic biochemical reactions in the body [14].

Zn radius can covalently bind to DNA [12,13]. Zn also plays an essential role in various cellular processes, including cell proliferation, differentiation, and apoptosis [14]. Several in vitro studies of Zn complexes have shown that the anti-cancer activity of Zn complexes is promising in reducing the growth of several cancers to avoid cytotoxic/tumor-suppressing effects on malignant cells [14]. The use of appropriate ligands can increase the biological activity of complex compounds [15]. Dithiocarbamate compounds can be used as radio-chemotherapeutic targeting agents in tumours [16–19]. Dithiocarbamate compounds and their derivatives are some of the useful metal-chelating antioxidants [20–23]. Dithiocarbamate complex has shown potential in stopping cell proliferation [24,25]. Dithiocarbamate compounds have an exceptional structure; namely, an S group can donate electrons monodentate and bidentate [26]. Dithiocarbamate ligands with the addition of oxygen and nitrogen donor groups (such as proline) can increase the diversity of the dithiocarbamate complex structure and affect the nature of the biological activity of the complex compound [27]. Hence, the present study synthesized, characterized physiochemical, and determined the anti-cancer activity through *in vitro* and *in silico* approaches.

2. Materials and methods

2.1. General

Carbon disulfide (99.5%), Cisplatin, Roswell Park Memorial Institute Medium, and DMSO, $ZnSO_4{\cdot}7H_2O$, Proline, Ethanol (95%), and Acetonitrile (95%) were purchased from Merck, USA.

2.2. Synthesis of Zn(ii)Prolinedithiocarbamate

Synthesis of Zn(II)Prolinedithiocarbamate was carried out through the synthesis of proline dithiocarbamate first. Proline (5 mmol) dissolved in minimum amount of ethanol. Carbon disulfide (5 mmol) was added slowly at 10 °C with constant stirring for 30 min. The proline dithiocarbamate solution was added ZnSO4·7H2O (3 mmol), dissolved in a minimum amount of ethanol, and stirred for 30 min. The precipitate formed was filtered and washed with ethanol and then recrystallized with acetonitrile and ethanol (1:2.v/v). The synthesis method is carried out by in situ method.

2.3. Zn(II)Prolinedithiocarbamate characterization

The melting point of the synthesized complex was determined using Electrothermal IA 9100, and A conductometer was used to measure the conductivity. The IR spectrum of the Zn(II) complex was analyzed by using the SHIMADZU Infrared Spectrophotometer using KBr pellets in the wavenumber range of 340–4000 cm^{-1}. Jenwey UV–Vis spectrophotometer at a wavelength of 200–1100 nm was used to obtain UV–Vis spectral data. Interactions between Zn and O, and S were also confirmed by XRD and computational NMR spectrum.

2.4. In vitro *study: cytotoxic test complex Zn(ii)Prolinedithiocarbamate against breast cancer cells (MCF-7)*

2.4.1. Media preparation/positive control/sample

Prepared liquid culture media Roswell Park Memorial Institute Medium (RPMI) complete. Set up positive controls to be used. The positive control used in this test is cisplatin. They dissolved the sample with a particular final concentration as stock. The solvent used is nontoxic to cells. The antiproliferative assay solution used was PrestoBlue™ Cell Viability Reagent.

2.4.2. Cell preparation

The cells used were confluent 70% min. Discarded media on the dish, then rinse the cell as much as 2x with 1 mL PBS. Added 1 mL of Trypsin-EDTA solution and then incrusted for 5 min so that the cell layer is dispersed (under an inverted microscope, the cell will appear to float. The cell is transferred to a tube that already contains media. Disenterfuge cells at a speed of 3000 rpm for 5 min. Discarded supernatant, then the pellets are dissolved into a tube containing media.

2.4.3. Treatment of cells with positive samples/controls/negative controls

Eight micro-tubes were prepared at 1.5 mL, micro-tubes were labelled with the appropriate dilution concentration, sample stock was diluted to eight concentration variations using solvent media. Removed 96 well plates that have contained cells from the incubator. It is labelled on the plate along the left margin, for which rows will be treated by standard and sampled lines. Then remove the media from each well. The 100 µL sample was transferred with a micropipette and a positive cisplatin control from a microtube to a 96-well plate containing cells. The steering wheel is incubated again for 48 h.

2.5. Absorbance measurement

9 mL of medium was prepared in a tube, then 1 mL of "PrestoBlue™ Cell Viability Reagent" was added (10 µL reagent for 90 µL media). The solution mixture of 100 µL was put into a microplate well and incubated for 1–2 h until a color change occurred.

PrestoBlue® reagent after entering into living cells will be reduced from the red compound resazurin with no intrinsic value to a red resorufin compound and high fluorescence. The conversion of values by the number of metabolically active cells can be measured quantitatively via the absorbance spectra of resazurin and resorufin) measured at a wavelength of 570 nm (reference: 600 nm) using a multimode reader.

2.6. Pharmacokinetics (Absorbtion, distribution, metabolism, excretion, toxicology/ ADME-Tox) prediction of Zn(ii)Prolinedithiocarbamate

The pharmacokinetic properties of Zn(II)Prolinedithiocarbamate were predicted using pKCSM tools [28]. Druglikeness of Zn(II)Prolinedithiocarbamate was expected to estimate the potential Zn(II)Prolinedithiocarbamate as drug. The drug-likeness prediction was carried out by SwissADME freely web-server [29].

2.7. In silico *study of Zn(ii)Prolinedithiocarbamate as anti-cancer*

Zn(II)Prolinedithiocarbamate was drawn and obtained the canonical SMILE with the online Cheminfo webserver (http://www.cheminfo.org/), then was modelled with online Corina to obtain a three-dimensional structure (https://www.mn-am.com/online_demos/corina_ demo). Complex compound receipts have interacted with the O(6)-methylguanine-DNA methyltransferase (MGMT) protein (PDB ID 1QNT) that was retrieved from Protein Databank. Molegro Virtual Docker 5 software was used to prepare the protein and back in docking between Zn(II)Prolinedithiocarbamate and O(6)-methylguanine-DNA methyltransferase (MGMT). MGMT protein was removed from unwanted ligands and cofactors than was predicted, and the binding cavities were based on the van der Waals parameter. Zn(II)Prolinedithiocarbamate was docked to

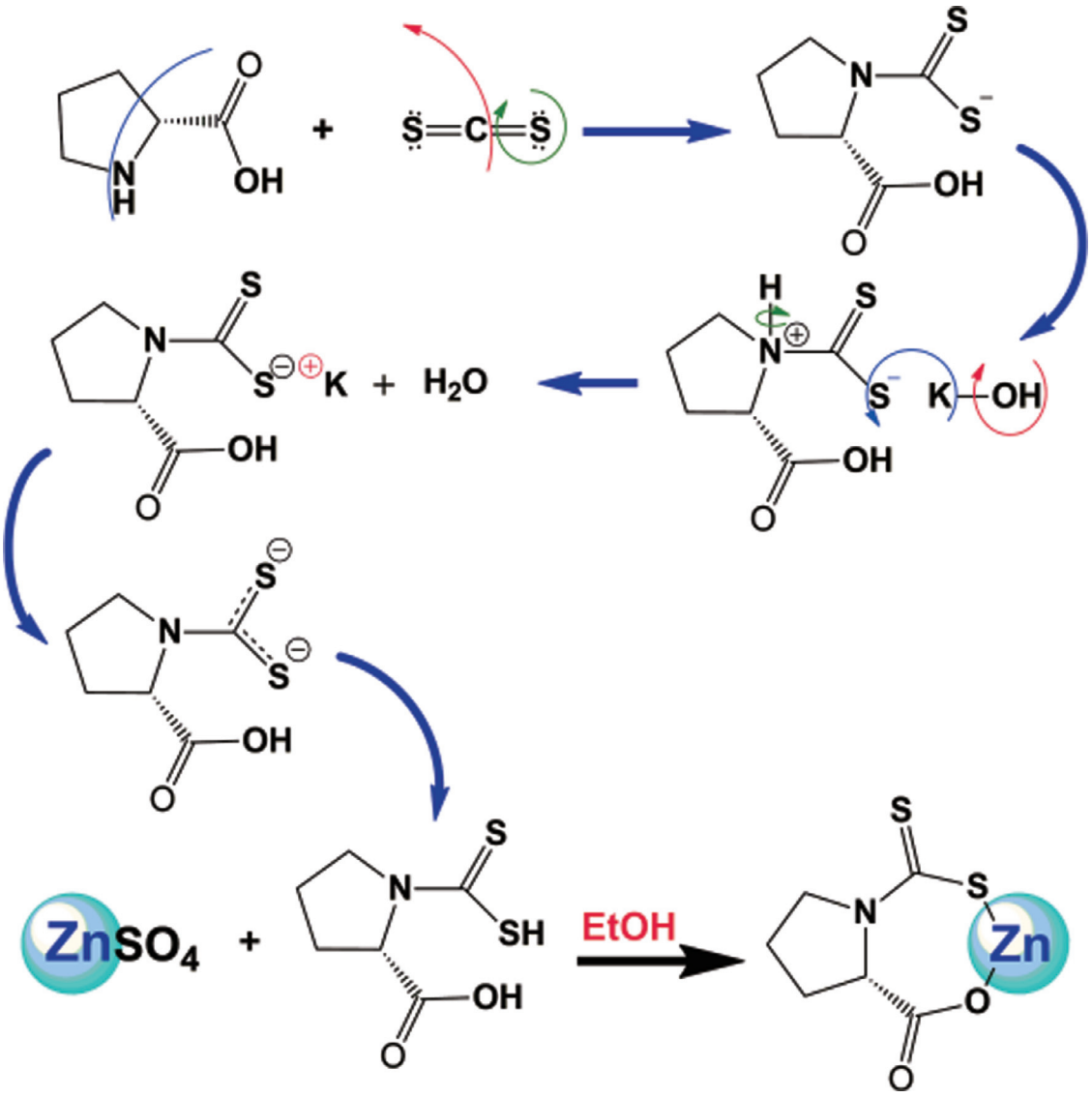

Fig. 1. Schematic illustration of the formation of complexes Zn(II)Prolinedithiocarbamate.

MGMT protein in specific grid $X = 1.29$A; $Y = 46.8$A; $Z = 55,6$A; Volume 35.84 A^3, and Surface 131.84 A^2, the radius was 15. Docking parameters are MolDock Score Grid 0.30A, MolDock Score, and Rerank score; the docking score indicates bond energy in kJ/mol units. The docking results are superimposed with proteins that have been predicted using PyMol software. Data is observed and analyzed with Discovery Studio ver 21.1.1. to get a 3D, 2D, and ligand binding area and target protein. Bonding energy is derived from the sum of The MolDock Score Grid, MolDock Score, and Rerank score and is averaged from five repeats and displayed with an average of ± Standard Deviation.

3. Results and discussion

3.1. Physiochemical characterization of Zn(ii)Prolinedithiocarbamate complex

The Zn(II)Prolinedithiocarbamate complex was successfully synthesized, the reaction of complex formation can be seen in Fig. 1 and performed high yield that was 68,13%. The complex showed a melting point at 284–286 °C. The Zn(II) complex was discovered to have a high purity level and to be stable above 200 °C and the conductivity was 0.02 mS/c, which means that the Zn(II) complex is a non-electrolyte compound.

When proline and carbon disulfide react, the carbocation formed on the carbon disulfide is attacked by electron-rich proline. The lone pair on proline's nitrogen atom will be used to form carbon disulfide bonds. After bonding, an unstable iminium ion is formed, and the iminium ion is stabilized by the addition of a base. KOH is the used as a base. The H^+ bound to the iminium ion will be attracted by the OH^- base, leaving it as a water molecule, while the K^+ will interact with the sulfide. The occurrence of electron resonance in the disulfide group will easily separate the apparent interaction between K^+ and sulfide ions. At the same time, adding $ZnSO_4$ to ethanol produces a complex compound called Zn(II)Prolinedithiocarbamate as the reaction's final product.

The resulting Zn(II)Prolineditiocarbamate complex can predict the bond length and bond angle of the metal with the ligand (Fig. 2). The Sn-S bond seems to show the characteristics of a covalent bond in such a way that the length of the Sn-S covalent bond ranges from 2143 A°, while the Sn-O bond is in the range of 1751 A°, where the O-Zn-S angle is 99.7°

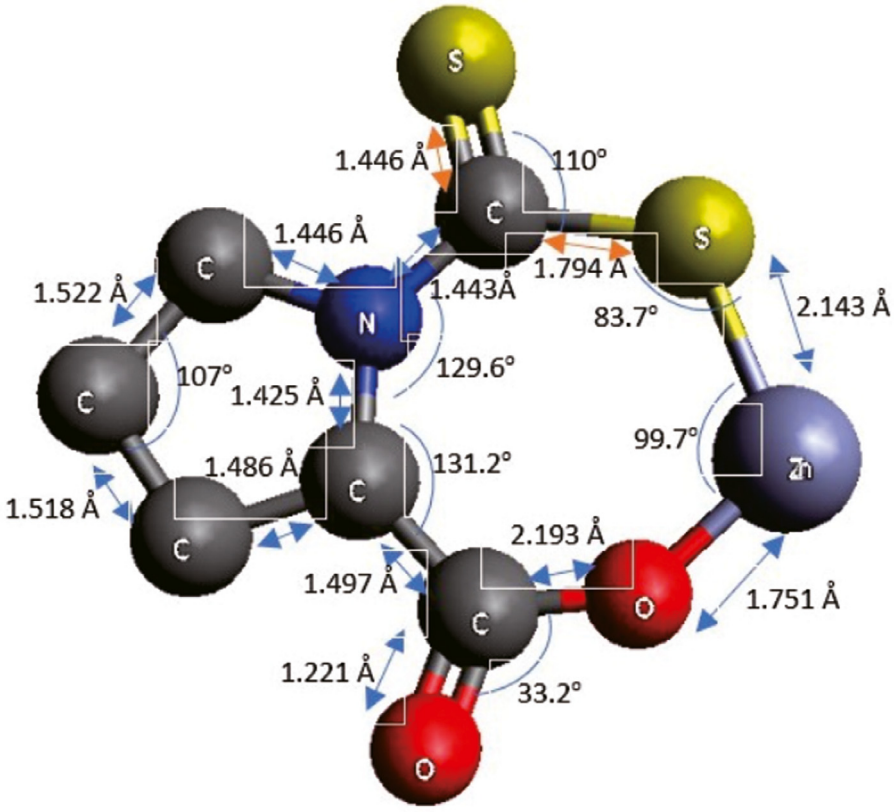

Fig. 2. Bond length and bond angle schematic of Complex Zn(II)Prolinedithiocarbamate.

Table 1
UV–Vis data of Zn(II)Prolinedithiocarbamate.

Compound	λ_{max} (nm)	Electronic Transition
Zn(II)Prolinedithiocarbamate	258 392	$\pi \rightarrow \pi^*$ $n \rightarrow \pi^*$

3.2. UV–Vis characterization

In complex compounds, changes in wavelength are caused by the presence of an auxochrome group, which is a saturated group with unbound electrons (free electrons) that, when attached to a chromophore group, causes the wave number to change. Strong bands originating from the $\pi \rightarrow \pi^*$ and $n \rightarrow \pi^*$ transitions can be seen in compounds containing the C=S group in the 250–320 range. According to the findings of a study on the dithiocarbamate complex by Bookhari et al., 1967, the band in the 310–400 region shows an electronic transition of intraligand $n \rightarrow \pi^*$ of the N=C=S group. For all dithiocarbamate complex compounds, the bands recorded in the UV region are generally the same, i.e. there are two main bands. Band 1 is a transition $\pi \rightarrow \pi^*$, while band II occurs when the metallic charge is transferred to the ligand [30].

The UV–Vis spectrophotometer reveals many wavelengths in the Zn(II)Prolinedithiocarbamate complex, as shown in Table 1. The spectra from UV VIS also performed specific characteristics of Zn(II)Prolinedithiocarbamate (Fig. 3). The Zn complex characterization in band 1 shows an absorption band at a wavelength of 258 nm, an intra ligand transition $\pi \rightarrow \pi^*$ of the CS2 group, which is influenced by the hyperconjugation effect of the R group on the nitrogen atom in the 250–300 nm absorption region. The shift in band II which is an intra ligand transition $n \rightarrow \pi^*$ of the N=C=S group at a wavelength of 392 nm, is shown in the Zn complex. The appearance of various other bands at the 470 nm absorption indicates the presence of a Charge Transfer (CT) transition between the metal and the ligand. Meanwhile, the appearance of absorption in the 525 nm region indicates the d orbital transition of the transition metal.

The hydrogen and carbon skeletons of the Zn(II)Prolinedithiocarbamate complex were identified using computational H–NMR and C–NMR spectra (Fig. 4). The ligand has bonded to the metal in the -O-Zn- bond. This is confirmed by the absence of a broad singlet proton signal from the OH carboxylic acid group in the region above 10 ppm. The methylene proton signal of the N-proline group of the dithiocarbamate moiety resonates in the range 1.54, 1.64; 1.95, 170 ppm [31] The hydrogen signal of the -CH–N group was found in the 2.8, 2.7 ppm region [32]. The carbon of the C=S group resonates in the downfield shift at 202.8 ppm [33]. The carbon atom of the cyclopentane ring bonded to nitrogen also resonates at a downward shift of 71.8 ppm. The downward shift occurs as a result of deshielding of the nitrogen atoms. The carbon atom attached to the nitrogen resonates at 52.2 ppm and the carbon atom of the cyclopentane attached to the carboxylate group resonates at 178.2 ppm. Another carbon atom of the cyclopentane ring assigned to the signal at 23.8, 27.9 ppm [34]

3.3. IR characterization

The infrared absorption peak of dithiocarbamate compounds revealed the presence of two types of bonds: C=N and C=S. There are two types of coordination in the absorption peak of (C-S), monodentate and bidentate. Bidentate coordination is indicated by single (C-S) absorption peaks, whereas monodentate coordination is indicated by double absorption peaks. Because the absorption of ν(C–N) occurs in the wave number between the single

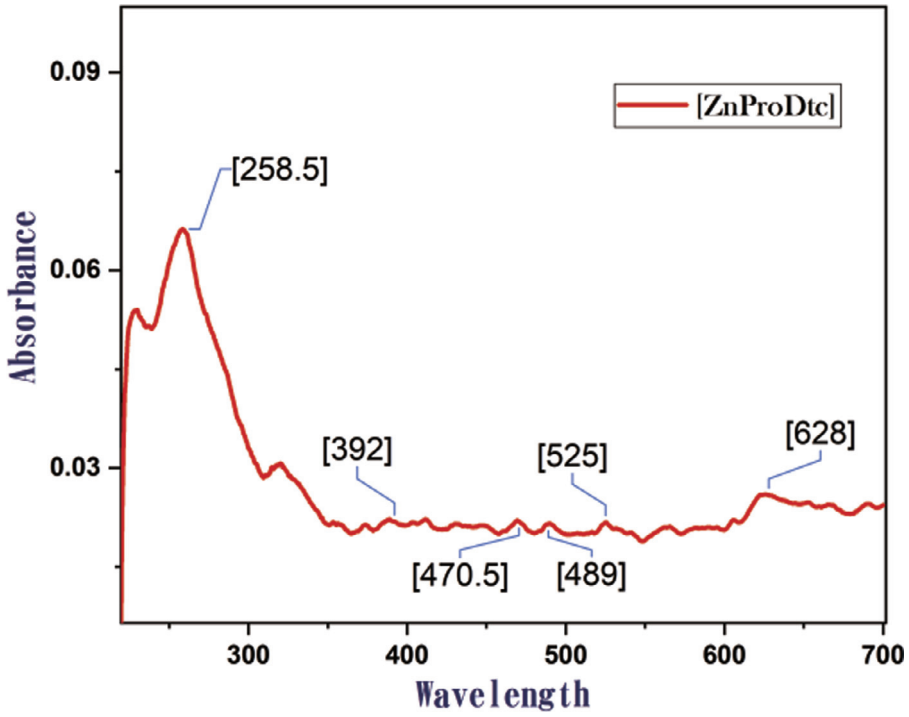

Fig. 3. UV–Vis Spectrum of Zn(II)Prolinedithiocarbamate.

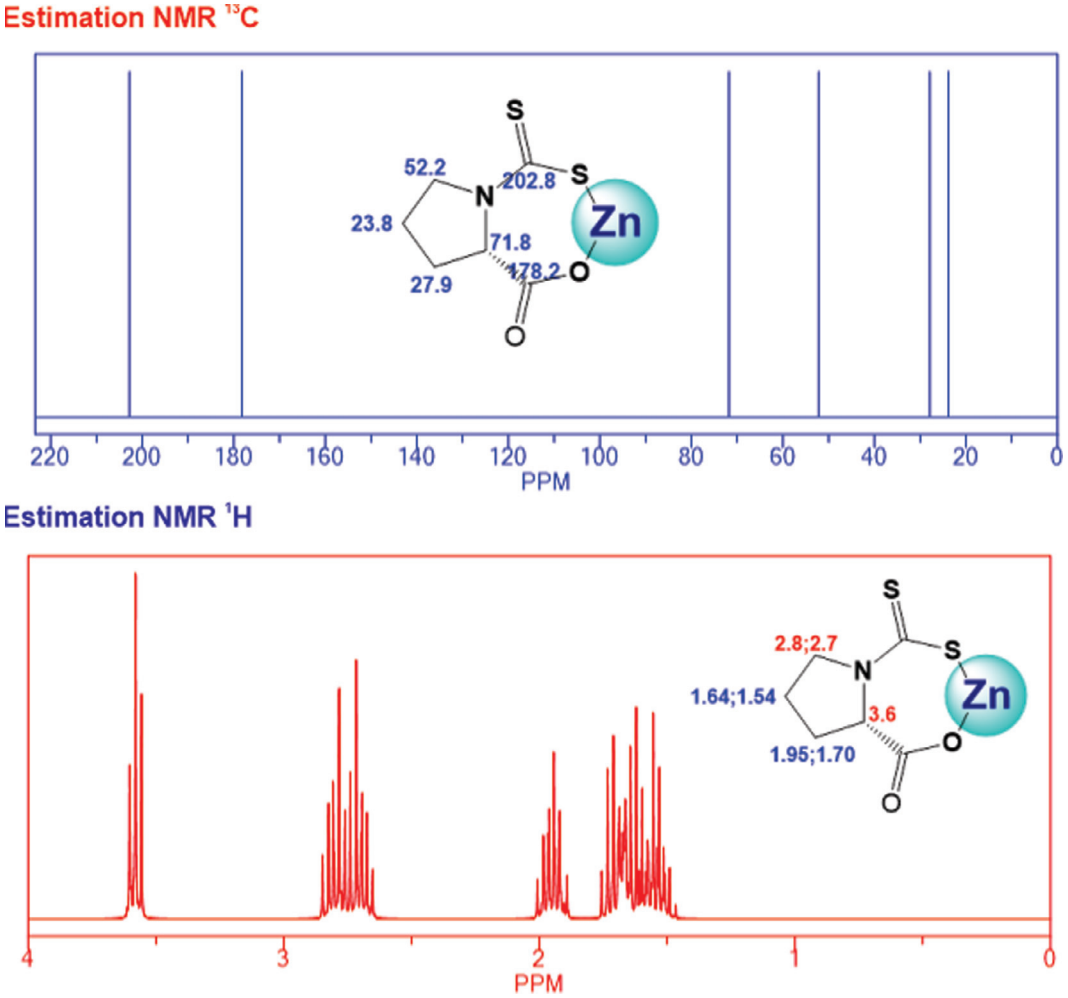

Fig. 4. computational H–NMR and C–NMR spectrum of Zn(II)Prolinedithiocarbamate.

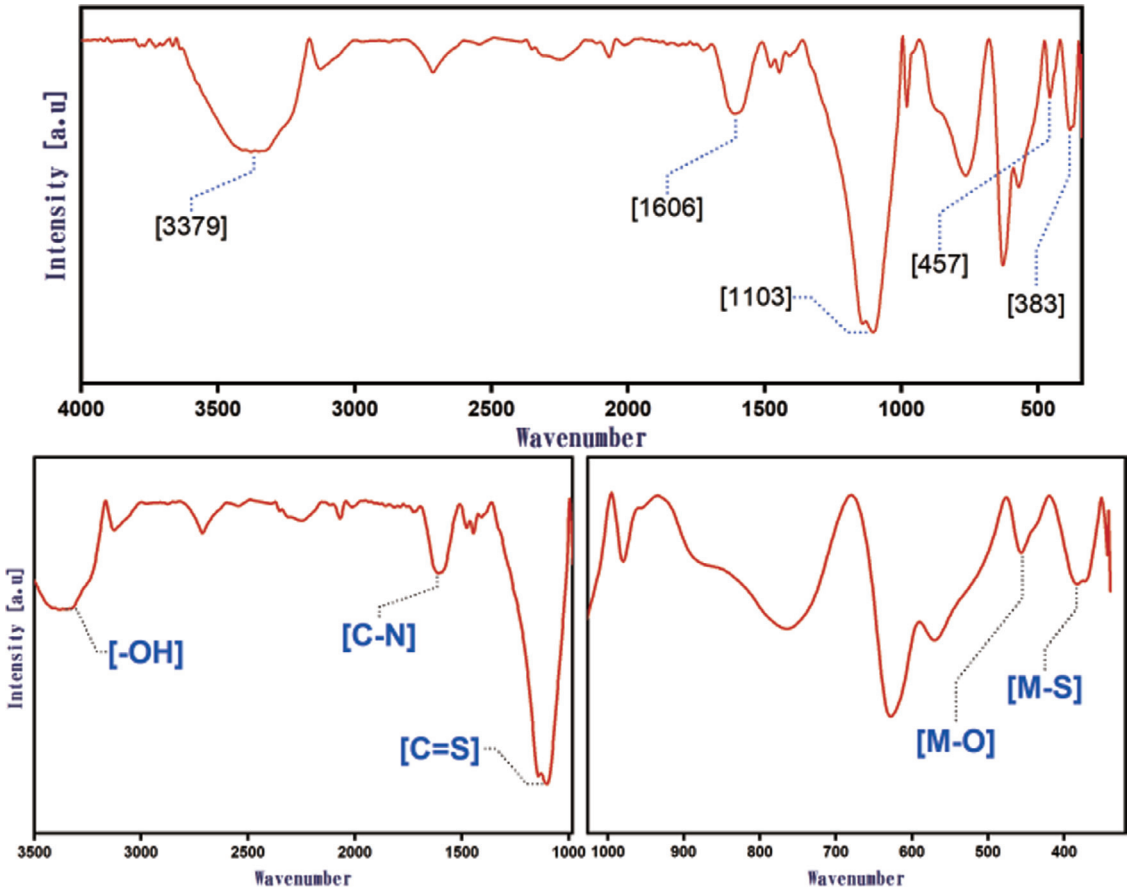

Fig. 5. IR Spectrum of Zn(II)Prolinedithiocarbamate.

Table 2
IR data of Zn(II)Prolinedithiocarbamate.

Compound	ν(C=N)	ν(C=S)	ν(M-S)	ν(M-O)
Zn(II) Prolinedithiocarbamate	1606 w	1103 s	383 m	457 w

s = strong; *m* = medium; *w* = weak.

bond (1350–1250) cm-1 and the double bond (1690–1640) cm-1 in the complex compound dithiocarbamate, the bond is written as ν(C=N). Furthermore, the C-S absorption is written as ν(C=S), with the wavelength number falling between the wavenumber of the C=S double bond (1050) and the wavelength number of the C=S double bond (1050) [35].

The resulting spectrum as shown in Table 2, the resulting spectrum can be used to identify the coordination link between the Zn metal and the ligand. The infrared spectrum of Zn(II) prolinedithiocarbamate has functional groups at wavenumbers 3379, 1606, 1103, 457, and 383 cm^{-1}, indicating the presence of OH, CN, CS, MO, and MS. (Fig. 5). The appearance of a peak around 3379 cm^{-1} was signed as a hydroxy–functional group (-OH) from water or ethanol solvents. The peak at 1606 cm^{-1} could be predicted as C=N group, and the peak at wavenumber 1103 cm^{-1} indicated C=S group. The infrared absorption peak at a wavenumber of 383 cm^{-1} suggests an interaction between the cation group (CS) and Zn metal ions. A wavenumber of 457 cm^{-1} was predicted from the interaction of the O atom of the complex compound with Zn. The functional group expressed on the IR spectra is related to the functional group in the proposed reaction of Zn(II)Prolinedithiocarbamate (Fig. 1). The vibrations of the ν(C-S), ν(C=N), and ν(MS) groups of the dithiocarbamate complex are strain vibrations [36], Others in the spectrum in the region between 383, 457 and 3379 cm^{-1} are associated with ν(MS), ν(MO) and ν(OH) are stretch vibrations, respectively [35].

3.4. XRD characterization

The Match 2 was used to analyze the XRD diffraction results of the complex compound Zn(II) Prolinedithiocarbamte (Fig. 6), which yielded two polycrystalline phases, zinc monosulfide (ZnS) and zinc monoxide (ZnO). The hexagonal structure of zinc monosulfide (ZnS) was identified as an X-ray diffraction peak with values of 2 29.59o; 40.89o; 42.43o; 44.12o; and 64.32o, with hkl values of 017; 117; 118; 119; and 217, according to data reported by Liu et al., 2009 [37]. The cubic structure of zinc monoxide (ZnO) was identified using X-ray diffraction peak values of 2 36.30o, 41.87o, 45.92o, and 61.18o, as well as hkl values of 111, 200, 311, and 202, as reported by Ali Khorsand Zak, 2011 [38].

3.5. Cytotoxicity studies on MCF-7 cells

The MTS test is a cytotoxicity test of Zn(II)Prolinedithiocarbamate complex against breast cancer cells (MCF-7). The cytotoxic assays of Zn complex and cisplatin were evaluated under the same conditions for comparison purposes. Treatment was carried out for 48 h for Zn complex and cisplatin against the MCF-7 cancer cell line, as shown in Table 3. The Zn complex compound against cancer cells used concentration variations ranging from the lowest 2.34 g/mL to the highest is 300 g/mL. The regression equation for the Zn(II)Prolinedithiocarbamate complex was obtained $y = -0.0013x + 0.7644$ (Fig. 7), and the regression equation

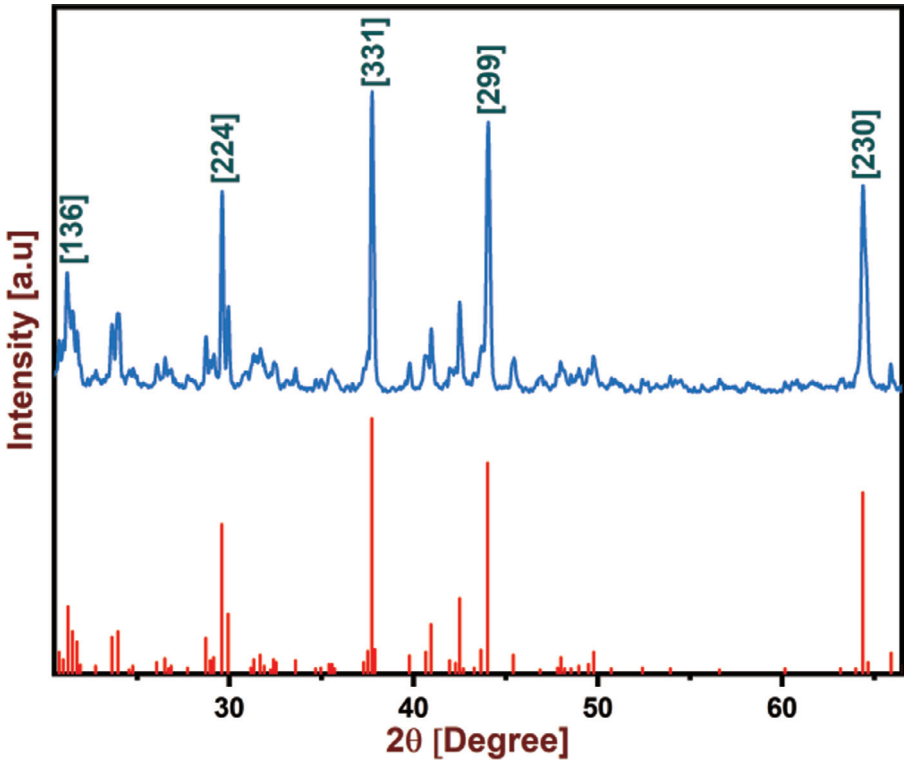

Fig. 6. XRD Spectrum of Zn(II)Prolinedithiocarbamate.

Table 3
IC_{50} values of the Zn(II)Prolinedithiocarbamate Complex.

Compounds	t(h)	IC_{50} (µg/mL)
Zn(II)Prolinedithiocarbamate	48	360,10
Cisplatin	48	53,48

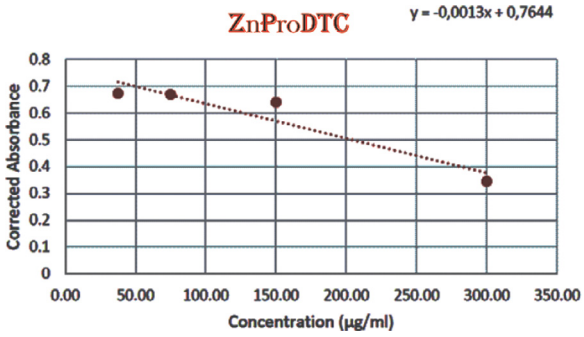

Fig. 7. Cytotoxicity Curve of Zn(II)Prolinedithiocarbamate.

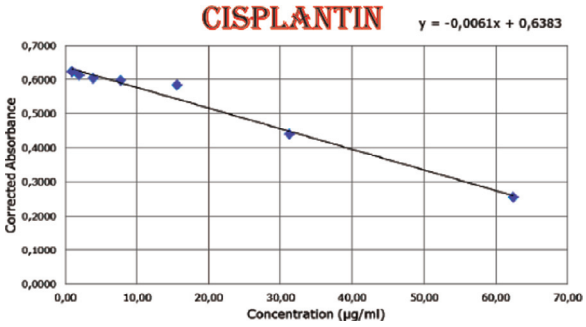

Fig. 8. Cytotoxicity Curve of Cisplatin.

of cisplatin $y = -0.0061x + 0.6383$ (Fig. 8). The regression equation was used to determine the IC_{50} value of the Zn complex and cisplatin. The IC_{50} value is obtained by replacing the y value with half the control value (DMSO). Documentation of the Zn(II)prolinedithiocarbamate well plate and the comparison of sample concentration with medium + cells, along the cisplatin side for MCF-7, are shown in Fig. S1 and Table S2. Apoptosis in MCF-7 cells of the Zn(II)Prolinedithiocarbamate and cisplatin complexes is illustrated in Fig. 9. At concentrations of the Zn(II)Prolinedithiocarbamate complex of 2.34–37.50 g/mL showed no visible cell death, apoptosis was initiated at concentrations 75 g/mL, By increasing the concentration of Zn (II) prolinedithiocarbamate complex, the apototic MCF-7 cancer cell line can be detected. Plasma membrane damage is a common cause of late apoptotic cells. Based on these morphological observations, the Zn complex promotes apoptosis in the MCF-7 cell line and treatment with cisplatin on MCF-7 cells showed a cytotoxic effect at a concentration of 53.48 g/mL MCF-7.

3.6. Pharmacokinetics prediction of Zn(ii)Prolinedithiocarbamate

Pharmacokinetics study involved absorption, distribution, metabolism, excretion, toxicity, and druglikeness of Zn(II)Prolinedithiocarbamate were described at Table 4. Zn(II)Prolinedithiocarbamate was absorbed 100% by intestine, and performed low absorption in water solubility and skin permeability. Caco2 permeability of Zn(II)Prolinedithiocarbamate was categorized as high value, which was higher than 0.90. VDss is a the steady state volume of distribution, indicating the total drug dose that distributed in the same concentration in blood plasma the VDss of Zn(II)Prolinedithiocarbamate was considered as low value and might did not performing renal failure and dehydration. In blood – brain barrier parameter of Zn(II)Prolinedithiocarbamate performed poorly distributed to the brain. In metabolism pa-

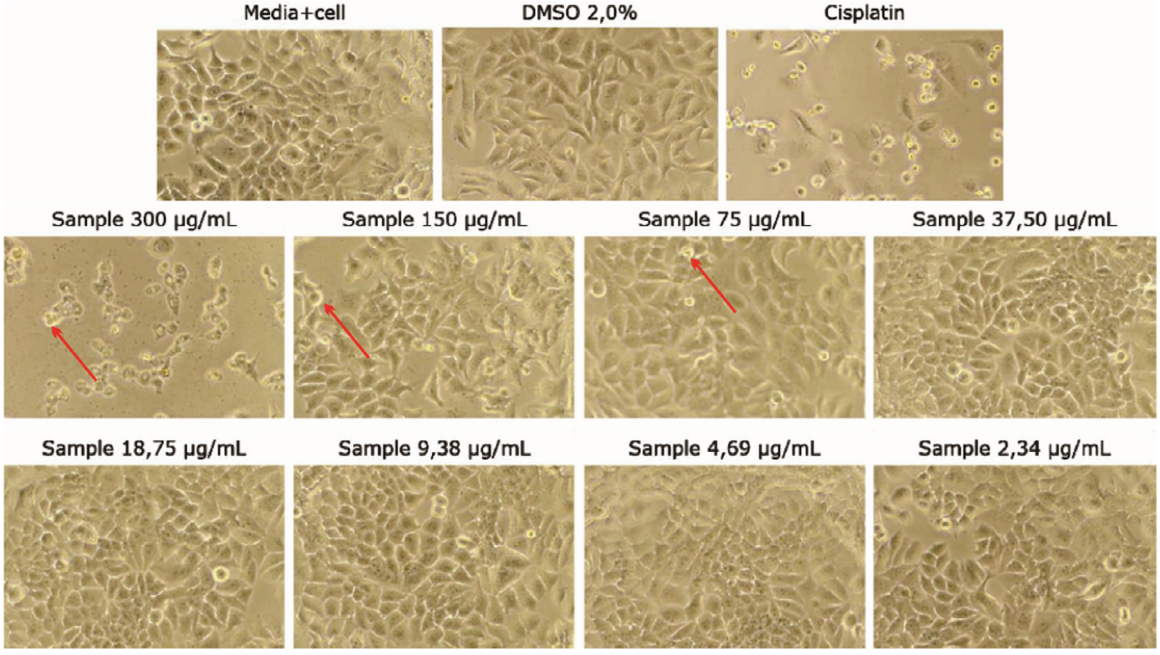

Fig. 9. Apoptosis of MCF-7 cells induced by Zn(II)Prolinedithiocarbamate.

Table 4
Pharmacokinetics prediction of the Zn(II)Prolinedithiocarbamate.

Parameter		Value	Parameter		Value
Absorption	Water Solubility (log mol/L)	−2563	**Excretion**	Total clearance (log ml/min/kg)	1187
	Caco2 permeability (log Papp in 10–6 cm/s)	1546		Renal OCT2 substrate	No
	Intestinal absorption (% absorbed)	100	**Toxicity**	AMES Toxicity	No
	Skin permeability (log Kp)	−2968		Max tolerated dose (log mg/kg/day)	0,871
	P-glycoprotein substrate	Yes		hERG II inhibitor	No
	P-glycoprotein I inhibitor	No		Oral Rat Acut Toxicity (LD50) (mol/kg)	2138
	P-glycoprotein II inhibitor	No		Oral Rat Chronic Toxicity (LOAEL) (log mg/kg_bw/day)	1216
Distribution	VDss (log L/kg)	−0,358		Hepatotoxicity	No
	Fraction unbound (Fu)	0,69		Skin Sensitisation	No
	BBB Permeability (log BB)	−0,255		*T. pyriformis toxicity (log ug/L)*	−0,059
	CNS permeability (log PS)	−3467		Minnow toxicity (log mM)	2329
Metabolism	CYP3A4 substrate	No	**Druglikeness**	Lipinski	Yes; 0 violation
	CYP1A2 inhibitor	No		Ghose	Yes
	CYP2C19 inhibitor	No		Veber	Yes
	CYP2C9 inhibitor	No		Egan	Yes
	CYP2D6 inhibitor	No		Muegge	Yes
	CYP3A4 inhibitor	No		Bioavaibility Score	0,55

rameters, the Zn(II)Prolinedithiocarbamate was not considered as substrate an inhibitors. Total clearance was high with the value was more than one and the zink complex was not as renal OCT2 substrate. The Zn(II)Prolinedithiocarbamate was not mutagenic complex, illustrating in negative value in AMES test, also not as hERG II inhibitor, not toxic in hepatocyte, and skin sensatisation. Druglikeness performed that the Zn(II)Prolinedithiocarbamate has potential as drug, according to the Lipinski, Ghose, Veber, Egan, and Muegge rules.

3.7. Zn(II)Prolinedithiocarbamate directly interact with O(6)-methylguanine-DNA methyltransferase (MGMT) protein

Zn(II)prolinedithiocarbamate interacts with MGMT proteins at several active site residues, including ARG147, LEU102, VAL106, ILE76, and GLU77 (Fig. 10). The two-dimensional ligand-protein interaction display shows several interactions, namely hydrogen bonding, metal acceptors, van der Waals, and Alkyl. The ligand-protein interaction resulted in -175 ± 11.7 kJ/mol binding energy, as shown in Table S1. Interestingly, Zn metal binds to two active sites of MGMT, LEU102, with a distance of 3.3A and VAL106, with a distance of 2.5A. Prolinedithiocarbamate ligands are also involved in binding to the active sites of ARG 147, ILE176, and GLU77. This indicates the effect of Proline dithiocarbamate ligands in increasing the biological activity of the Zn complex. The active site of the compound-complex against the MGMT protein shows binding to active DNA sites that affect the DNA methylation process.

Synthetic Zn(II)Prolinedithiocarbamate was performed high degree of purity with high conductivity and showed a non-electrolyte compound. Based on the IR and UV–Vis spectra, Zn(II)Prolinedithiocarbamate was successfully synthesized. In vitro and in silico study revealed that Zn(II)Prolinedithiocarbamate induced apoptosis in MCF-7 cell lines and exhibited a potential MGMT inhibitor. O(6)-methylguanine-DNA methyltransferase (MGMT) protein is an enzyme that repairs the pre-carcinogenic, pre-mutagenic DNA damage. The MGMT protein expressed responses from the alkylating environment and methylating agent [39]. MGMT protein repairs the damaged DNA by catalyzing the methyl transfer from the O6 site of guanine to the cysteine [40]. The repairing process prevented gene mutations that were regulated by epigenetic. Previous studies explored the MGMT inhibitors for glioblastoma therapy. Inhibition of MGMT protein was reported

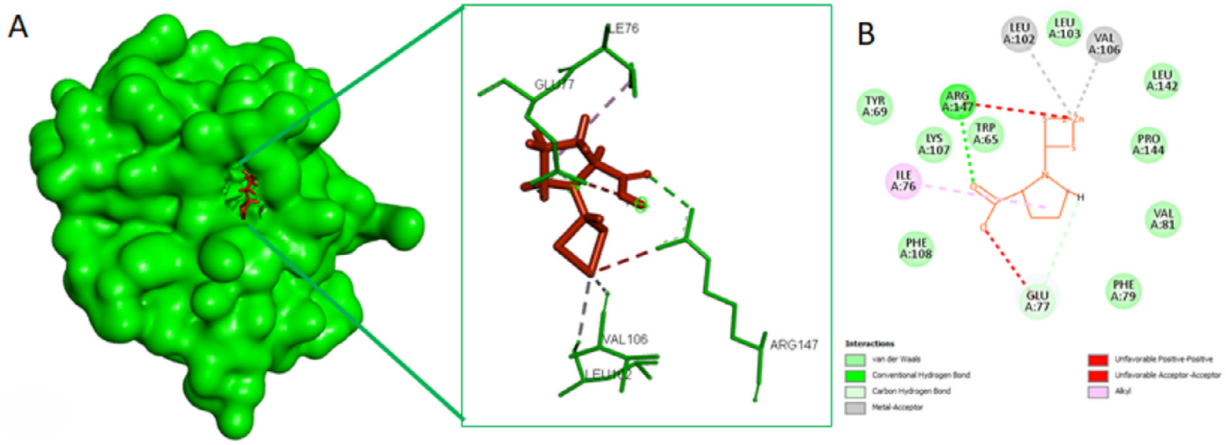

Fig. 10. The binding pose of Zn(II)Prolinedithiocarbamate - O(6)-methylguanine-DNA methyltransferase (MGMT) protein, green color performed O(6)-methylguanine-DNA methyltransferase (MGMT) protein, the red color showed Zn(II)Prolinedithiocarbamate. A. The overview of Zn(II)Prolinedithiocarbamate - O(6)-methylguanine-DNA methyltransferase (MGMT) complex, B. 2D view of Zn(II)Prolinedithiocarbamate - O(6)-methylguanine-DNA methyltransferase (MGMT) complex, C. The detailed interaction of ligand-protein interaction.

to enhance alkylating agent-induced apoptosis in cancer cells [41]. Besides, Lechapt-Zalcman, 2012 [42] said repressing the overexpression of MGMT protein reduced the glioblastoma performance. The current study performed that Zn(II)Prolinedithiocarbamate directly interacts with O(6)-methylguanine-DNA methyltransferase (MGMT) residues, indicating the metal complex might reducing the MGMT activity. Chikan et al. (2015) described the MGMT structure and functional domain of MGMT. The functions were DNA docking, base flipping and DNA docking, metal binding and active site of MGMT. Residues identified as DNA binding proteins were Lys125, Asn123, Phe94, Ser93, Tht95, and Arg135. Protein base flipping domains were identified on Ser/Ile151, Tyr114, Gln115, and Cys145 residues. The metal binding MGMT was performed on His29, Cys24, and His85. However, the reported active residues were not detected in the present study; Zn (II)Prolinedithiocarbamate probably altered the conformation of MGMT protein structure [43].

The synthesized complex was tested for cytotoxicity against breast cancer cells (MCF-7) in vitro and compared with the anticancer activity of cisplatin, which is the most commonly used drug today and is known to be active against breast cancer cells (MCF-7). The results of the IC_{50} values of the Zn(II) ProlineDithiocarbamate complex and cisplatin (treatment time for 48 h) are shown in Table 3. These results indicate the IC_{50} value of the Zn(II) complex has a strong correlation with cisplatin. IC_{50} cisplatin = 53.48 g/mL while the Zn(II) complex is IC_{50} = 360.10 g/mL, so the Zn(II) complex can be declared active against cancer cells.

Prayong (2008) classifies the IC50 standard cytotoxic samples into three categories, namely 1–100 g/mL high cytotoxicity, 100–1000 g/mL moderate, and 1000 g/mL weak or even nontoxic to cancer cells [44]. The complex has cytotoxicity on MCF-7 cancer cells seen from the nature of metal bioactivity in the body and the structure of the complex. The Zn complex showed good cytotoxicity to cancer cells because the HSAB properties of Zn(II) belonged to the acid category, and nitrogen from guanine, which was the basic framework of DNA structure, was included in the borderline base category to allow a strong bond. There is a strong relationship between the Zn(II) complex and the nitrogenous bases of the basic framework of DNA structure. Interestingly, this interaction disrupts the electronic structure of guanine in the base pair in the DNA duplex triggered by $H^+$and the Zn transition metal ion. When positive ions interact with pyridine-type nitrogen (G–N7) (Fig. 11), the unbonded electron pair located in the sp^2 hybrid orbital can overlap significantly with the p-electronic system of the indole guanine ring, inducing a decrease in the electronic density of the ring, including the endocyclic N1 nitrogen atom [45]. This corresponds to the metal lanthanides (Tb and Eu) bonded to the nitrogen atom of the DNA nucleotide [46,47]. The interaction of the Zn(II)Prolinedithiocarbamate complex with DNA was confirmed by molecular docking. The Zn(II) complex can be attributed to the function of the Zn complex as a competitive inhibitor of Heme Oxygenase (HMOX1), which is produced in large quantities in solid tumors [48].

Metal complexes with DNA are covalently coordinated in coordination with various specific geometries [49]. In addition, metal complexes can also sneak into DNA gaps. Most of these reactions occur in complexes containing aromatic heterocyclic ligands [50]. Metal complex interactions with DNA can occur through covalent bonds or non-covalently. The simplest form of the first non-covalent interaction is electrostatic interaction or outside binding. This interaction occurs between metal complexes such as positively charged metal complexes and the partially negatively charged outer skeleton (phosphate) of DNA. Interactions can occur on the outside of the DNA double helix. An example of this interaction is the sodium and magnesium cations with the outer DNA phosphate. The second type of interaction is groove binding. This interaction is strongly influenced by the geometry of the complex compounds that will interact with DNA and the electric field around the DNA framework, van der Waals forces, hydrogen bonds and hydrophobic effects. [51]. According to Balasubramanian's research [52] chemicals that bind strongly with DNA can suppress telomerase and influence the transcription of particular oncogenes.

In fact, the purine nucleobase N7 is the favored binding site in DNA [53]. Fig. S2 depicts a schematic with all possible binding locations. N3 is sterically inhibited in double-stranded DNA, leaving only N7 (bold arrow in Fig. S2). N1 from adenine and N3 from cytosine can also attach to Zn complexes in single-stranded DNA (dotted arrows in Fig. S2). Because protonated purine and pyrimidine nitrogen atoms in the aromatic π system contain a delocalized lone pair of electrons, they are only available for coordination of Zn complexes after deprotonation (empty arrows in Fig. S2). The kinetic energy of guanine bonds is higher [54]. The higher basicity of nitrogen causes this propensity. The DNA structure has been severely altered, resulting in lower melting temperatures, shortening, detachment, and denaturation. The MCF-7 cell morphology revealed that the Zn(II)-DNA complex reaction disrupted cell cycle progression.In circumstances of insufficient repair, the cell will eventually experience a failed attempt at mitosis, resulting in apoptotic cell death.

Intercalation occurs when planar heteroatomic compounds penetrate the DNA pair gap and interact perpendicular to the DNA double helix axis. Unlike the previous two types of interactions, this type requires a conformational change (distortion) of the DNA framework to make room for the incoming molecule. Generally, base pairs in adjacent DNA will distance themselves to allow sufficient space for the entry of planar aromatic intercalators. This kind of process causes stretching of the DNA double helix structure, which results in changes in electron density in the phosphate framework and changes in DNA sugar conformation. An example of an interaction involving the intercalation of ligands into DNA base pairs is the intercalation of ethidium bromide (EB) and diazapyrenium dichloride (DAP) into DNA base pairs. The ligand will react with the functional group found in the DNA groove [55]. The dithiocarbamate ligand has made a significant contribution to the cytotoxicity of the Zn complexes of the cancer cells tested. Ligands serve as carriers and contribute to the lipophilicity of the complex and can facilitate the movement of metals to cell sites [56].

4. Conclusions

A novel Zn(II) Prolineditiocarbamate complex has been successfully synthesized and described, which involves the interaction of proline and carbon disulfide (CS2) in ethanol, as well as Zn metal in the form of a salt. The structure and content of the synthesized complex were validated by spectroscopic and computational data. The dithiocarbamate ligand is monodentately coupled to the zinc atom. Molecular docking was used to demonstrate the interaction of the Zn(II) prolinedithiocarbamate complex with DNA from MCF-7 strain cells.At an IC50 of 360.10 µg/mL, cytotoxicity of Zn(II) prolinethiocarbamate against the MCF-7 cell line revealed changes in cancer cell morphology. Potential Zn(II) prolinedithiocarbamate complex compounds could pave the way for the development of MCF-7-specific chemotherapy drugs.

Declaration of Competing Interest

The authors declare that they have no known competing financial interests or personal relationships that could have appeared to influence the work reported in this paper.

CRediT authorship contribution statement

Rizal Irfandi: Conceptualization, Methodology, Investigation, Writing – original draft. **Santi Santi:** Visualization, Data curation. **Indah Raya:** Conceptualization, Methodology, Supervision. **Ahyar Ahmad:** Writing – review & editing, Validation. **Ahmad Fudholi:** Writing – review & editing. **Dewi Ratih Tirto Sari:** Formal analysis, Software.

Acknowledgment

We would like to thank LPDP (Institute for Education Fund Management) as the funder

Supplementary materials

Supplementary material associated with this article can be found, in the online version, at doi:10.1016/j.molstruc.2021.132101.

References

[1] A. Adjiri, DNA mutations may not be the cause of cancer, Oncol. Ther. 5 (1) (2017) 85–101.
[2] M.R. Stratton, P.J. Campbell, P.A. Futreal, The cancer genome, Nature 458 (7239) (2009) 719–724.
[3] M. Shareef, M.A. Ashraf, M. Sarfraz, Natural cures for breast cancer treatment, Saudi Pharm. J. 24 (3) (2016) 233–240.
[4] I.S.J. Ferlay, R. Dikshit, S. Eser, C. Mathers, M. Rebelo, et al., Cancer incidence and mortality worldwide: sources, methods and major patterns in GLOBOCAN 2012, Int. J. Cancer 136 (2014) 29.
[5] L. Xu, Z. Chu, H. Wang, L. Cai, Z. Tu, H. Liu, et al., Electrostatically assembled multilayered films of biopolymer enhanced nanocapsules for on-demand drug release, ACS Appl. Bio Mater. 2 (8) (2019) 3429–3438.
[6] L. Xu, H. Wang, Z. Chu, L. Cai, H. Shi, et al., Temperature-responsive multilayer films of micelle-based composites for controlled release of a third-generation EGFR inhibitor, ACS Appl. Polym. Mater. 2 (2) (2020) 741–750.
[7] W.G. Lu, L. Jiang, X.L. Feng, T.B. Lu, Three 3D coordination polymers constructed by Cd (II) and Zn (II) with imidazole-4, 5-dicarboxylate and 4, 4 '-bipyridyl building blocks, Cryst. Growth Des. 6 (2) (2006) 564–571.
[8] N. Hadjiliadis, E. Sletten, Metal Complex-DNA Interactions, John Wiley & Sons, 2009.
[9] A. Dorcier, W.H. Ang, S. Bolano, L. Gonsalvi, et al., In vitro evaluation of rhodium and osmium RAPTA analogues: the case for organometallic anticancer drugs not based on ruthenium, Organometallics 25 (17) (2006) 4090–4096.
[10] Y. Li, T. Jun, W. Bo-Chu, Z.H.U. Lian-Cai, Synthesis, characterization, and anti–cancer activity of emodin-Mn (II) metal complex, Chin. J. Nat. Med. 12 (12) (2014) 937–942.
[11] J.O. Adeyemi, D.C. Onwudiwe, Organotin (IV) dithiocarbamate complexes: chemistry and biological activity, Molecules 23 (10) (2018) 2571.
[12] F. Arjmand, S. Parveen, D.K. Mohapatra, Synthesis, characterization of Cu (II) and Zn (II) complexes of proline-glycine and proline-leucine tetrapeptides: in vitro DNA binding and cleavage studies, Inorgan. Chim. Acta 388 (2012) 1–10.
[13] P. Prihantono, R. Irfandi, I. Raya, The comparison of Zn (II) arginine dithiocarbamate cytotoxicity in T47D breast cancer and fibroblast cells, Breast Dis. (2021) 1–7 Preprint.
[14] P.A. Vigato, S. Tamburini, L. Bertolo, The development of compartmental macrocyclic Schiff bases and related polyamine derivatives, Coord. Chem. Rev. 251 (11–12) (2007) 1311–1492.
[15] I. Ritacco, N. Russo, E. Sicilia, DFT investigation of the mechanism of action of organoiridium (III) complexes as anticancer agents, Inorg. Chem. 54 (22) (2015) 10801–10810.
[16] S.Z. Khan, M.K. Amir, R. Abbasi, M.N. Tahir, Zia-ur-Rehman, New 3D and 2D supramolecular heteroleptic palladium (II) dithiocarbamates as potent anticancer agents, J. Coord. Chem. 69 (20) (2016) 2999–3009.
[17] M. Altaf, M. Monim-ul-Mehboob, A.N. Kawde, et al., New bipyridine gold (III) dithiocarbamate-containing complexes exerted a potent anticancer activity against cisplatin-resistant cancer cells independent of p53 status, Oncotarget 8 (1) (2017) 490.
[18] J.S. Bang, H.M. Choi, H.I. Yang, et al., Fetal bovine serum requirement for pyrrolidine dithiocarbamate-induced apoptotic cell death of MCF-7 breast tumor cells, Eur. J. Pharmacol. 649 (1–3) (2010) 135–139.
[19] S. Mollin, R. Riedel, K. Harms, E. Meggers, Octahedral rhodium (III) complexes as kinase inhibitors: control of the relative stereochemistry with acyclic tridentate ligands, J. Inorg. Biochem. 148 (2015) 11–21.
[20] L. Malaguarnera, M.R. Pilastro, R. DiMarco, et al., Cell death in human acute myelogenous leukemic cells induced by pyrrolidinedithiocarbamate, Apoptosis 8 (5) (2003) 539–545.
[21] D. Buac, S. Schmitt, G. Ventro, F. Rani Kona, Q. Ping Dou, Dithiocarbamate-based coordination compounds as potent proteasome inhibitors in human cancer cells, Mini Rev. Med. Chem. 12 (12) (2012) 1193–1201.
[22] A. Boschi, P. Martini, L. Uccelli, 188Re (V) nitrido radiopharmaceuticals for radionuclide therapy, Pharmaceuticals 10 (1) (2017) 12.
[23] A. Boschi, L. Uccelli, P. Martini, A picture of modern Tc-99 m radiopharmaceuticals: production, chemistry, and applications in molecular imaging, Appl. Sci. 9 (12) (2019) 2526.
[24] E.A. Hassan, S.E. Zayed, Dithiocarbamates as precursors in organic chemistry; synthesis and uses, Phosphorus Sulfur Silicon Relat. Elem. 189 (3) (2014) 300–323.
[25] R.Irfandi Prihantono, I. Raya, Warsinggih, Potential anticancer activity of Mn (II) complexes containing arginine dithiocarbamate ligand on MCF-7 breast cancer cell lines, Ann. Med. Surg. 60 (2020) 396–402.
[26] I. Rogachev, V. Gusis, A. Gusis, et al., Spectrophotometric determination of copper complexation properties of new amphiphilic dithiocarbamates, React. Funct. Polym. 42 (3) (1999) 243–254.
[27] I.P. Ferreira, G.M. de Lima, E.B. Paniago, et al., Study of metal dithiocarbamate complexes, Part V. Metal complexes of [S2CN (CH2CH (OMe) 2]: a standard dimeric zinc dithiocarbamate structural motive, a rare cadmium dithiocarbamate coordination polymer, and a hydrated sodium dithiocarbarmate complex, with a [Na_2O_2] core and chain, Inorgan. Chim. Acta 441 (2016) 137–145.
[28] D.E. Pires, T.L. Blundell, D.B. Ascher, pkCSM: predicting small-molecule pharmacokinetic and toxicity properties using graph-based signatures, J. Med. Chem. 58 (9) (2015) 4066–4072.
[29] A. Daina, O. Michielin, V. Zoete, SwissADME: a free web tool to evaluate pharmacokinetics, drug-likeness and medicinal chemistry friendliness of small molecules, Sci. Rep. 7 (1) (2017) 1–13.
[30] A.K. Mishra, N. Manav, N.K. Kaushik, Organotin (IV) complexes of thiohydrazones: synthesis, characterization and antifungal study, Spectrochim. Acta Part A Mol. Biomol. Spectrosc. 61 (13–14) (2005) 3097–3101.
[31] B.A. Prakasam, K. Ramalingam, R. Baskaran, et al., Synthesis, NMR spectral and single crystal X-ray structural studies on Ni (II) dithiocarbamates with NiS2PN, NiS2PC, NiS2P2 chromophores: crystal structures of (4-methylpiperazinecarbodithioato)(thiocyanato-N)(triphenylphosphine) nickel (II) and bis (triphenylphosphine)(4-methylpiperazinecarbodithioato) nickel (II) perchlorate monohydrate, Polyhedron 26 (5) (2007) 1133–1138.

[32] F. Shaheen, M. Sirajuddin, S. Ali, et al., Organotin (IV) 4-(benzo [d][1, 3] dioxol-5-ylmethyl) piperazine-1-carbodithioates: synthesis, characterization and biological activities, J. Organomet. Chem. 856 (2018) 13–22.
[33] R. Sharma, M. Nagar, M. Agarwal, H. Sharma, Synthesis, characterization and antimicrobial activities of some mixed ligand complexes of Co (II) with thiosemicarbazones and N-protected amino acids, J. Enzyme Inhib. Med. Chem. 24 (1) (2009) 197–204.
[34] L.V. Kumar, G.R. Nath, Synthesis and Characterization Studies of Cobalt (II), Nickel (II), Copper (II) and Zinc (II) Complexes of Carboxymethyl-N-Methyl-N-Phenyl Dithiocarbamate, Orient. J. Chem., 34 (6) (2018) 3064.
[35] J.O. Adeyemi, G.M. Saibu, L.O. Olasunkanmi, et al., Synthesis, computational and biological studies of alkyltin (IV) N-methyl-N-hydroxyethyl dithiocarbamate complexes, Heliyon 7 (8) (2021) e07693.
[36] N. Muhammad, S. Ali, I.S. Butler, A. Meetsma, New mononuclear organotin (IV) 4-benzhydrylpiperazine-1-carbodithioates: synthesis, spectroscopic characterization, X-ray structures and in vitro antimicrobial activities, Inorgan. Chim. Acta 373 (1) (2011) 187–194.
[37] S. Liu, H. Zhang, M.T. Swihart, Spray pyrolysis synthesis of ZnS nanoparticles from a single-source precursor, Nanotechnology 20 (23) (2009) 235603.
[38] A.K. Zak, R. Razali, W.H. Abd Majid, M. Darroudi, Synthesis and characterization of a narrow size distribution of zinc oxide nanoparticles, Int. J. Nanomed. 6 (2011) 1399.
[39] W. Yu, L. Zhang, Q. Wei, A. Shao, O6-methylguanine-DNA methyltransferase (MGMT): challenges and new opportunities in glioma chemotherapy, Front. Oncol. 9 (2020) 1547.
[40] M. Christmann, B. Verbeek, W.P. Roos, B. Kaina, O6-Methylguanine-DNA methyltransferase (MGMT) in normal tissues and tumors: enzyme activity, promoter methylation and immunohistochemistry, Biochim. Biophys. Acta (BBA) Rev. Cancer 1816 (2) (2011) 179–190.
[41] C.H. Fan, W.L. Liu, H. Cao, et al., O6-methylguanine DNA methyltransferase as a promising target for the treatment of temozolomide-resistant gliomas, Cell Death Dis. 4 (10) (2013) e876.
[42] E. Lechapt-Zalcman, G. Levallet, A.E. Dugue, A. Vital, et al., O6-methylguanine-DNA methyltransferase (MGMT) promoter methylation and low MGMT-encoded protein expression as prognostic markers in glioblastoma patients treated with biodegradable carmustine wafer implants after initial surgery followed by radiotherapy with concomitant and adjuvant temozolomide, Cancer 118 (18) (2012) 4545–4554.
[43] N.A. Chikan, S. Bukhari, N. Shabir, et al., Atomic insight into the altered O6-Methylguanine-DNA methyltransferase protein architecture in gastric cancer, PLoS ONE 10 (5) (2015) e0127741.
[44] P. Prayong, S. Barusrux, N. Weerapreeyakul, Cytotoxic activity screening of some indigenous Thai plants, Fitoterapia 79 (7–8) (2008) 598–601.
[45] X. Cui, J. Qi, H. Tan, F. Chen, Comparison of ancient and modern Chinese based on complex weighted networks, PLoS ONE 12 (11) (2017) e0187854.
[46] S. Santi, A.W. Wahab, I. Raya, A. Ahmad, M. Maming, Synthesis, spectroscopic (FT-IR, UV–visible) study, and HOMO-LUMO analysis of adenosine triphosphate (ATP) doped trivalent terbium, J. Mol. Struct. 1237 (2021) 130398.
[47] A.W.Wahab Santi, I. Raya, A. Ahmad, Synthesis and interaction of adenosine-5′-triphosphate with rare earth metal Europium (Eu^{3+}), AIP Conf. Proce. 2296 (1) (2020) 020074.
[48] R. Huang, A. Wallqvist, D.G. Covell, Anticancer metal compounds in NCI's tumor-screening database: putative mode of action, Biochem. Pharmacol. 69 (7) (2005) 1009–1039.
[49] J. Anastassopoulou, Metal–DNA interactions, J. Mol. Struct. 651 (2003) 19–26.
[50] K.L. Berkner, W.R. Folk, Polynucleotide kinase exchange reaction, J. Biol. Chem 252 (3) (1977) I76–3184.
[51] S.N. Georgiades, N.H. Abd Karim, K. Suntharalingam, R. Vilar, Interaction of metal complexes with G-quadruplex DNA, Angew. Chem. Int. Ed. 49 (24) (2010) 4020–4034.
[52] J. Dash, P.S. Shirude, S. Balasubramanian, G-quadruplex recognition by bis-indole carboxamides, Chem. Commun. (26) (2008) 3055–3057.
[53] S. Ishida, J. Lee, D.J. Thiele, I. Herskowitz, Uptake of the anticancer drug cisplatin mediated by the copper transporter Ctr1 in yeast and mammals, Proc. Natl. Acad. Sci. 99 (22) (2002) 14298–14302.
[54] F.A. Blommaert, H.C. van Dijk-Knijnenburg, F.J. Dijt, L. den Engelse, R.A. Baan, F. Berends, A.M.J. Fichtinger-Schepman, Formation of DNA adducts by the anticancer drug carboplatin: different nucleotide sequence preferences in vitro and in cells, Biochemistry 34 (26) (1995) 8474–8480.
[56] V. Luzzati, F. Masson, L.S. Lerman, Interaction of DNA and proflavine: a small-angle x-ray scattering study, J. Mol. Biol. 3 (5) (1961) 634–639.
[57] N.F. Kamaludin, N. Awang, I. Baba, A. Hamid, C.K. Meng, Synthesis, characterization and crystal structure of organotin (IV) N-butyl-N-phenyldithiocarbamate compounds and their cytotoxicity in human leukemia cell lines, Pak. J. Biol. Sci. PJBS 16 (1) (2013) 12–21.